

Equivalent Combinations of Discharge Capacitor Bank and Multi-Turn Coil in Magnetic Pulse Welding of Al/Cu Sheets

Tomokatsu AIZAWA

Tokyo Metropolitan College of Technology 1-10-40, Higashi-Ohi, Shinagawa-ku, Tokyo 140-0011, Japan

E-mail: aizawa@mem.iee.or.jp

Abstract Magnetic pulse welding of overlapped Al/Cu sheets is performed by flowing a discharge current from a capacitor bank to a flat coil. By increasing the number of coil turns, it is possible to further reduce the discharge current required for welding. In order to make each rise time of the current as equal as possible, the discharge bank capacity is selected as 24, 6 and 1.5 μF for the 4, 8 and 16-turn coils respectively. Based on the experimental results using the 4 and 8-turn coils, we will compare and examine such combinations of bank capacity and coil turn number. When the discharge energy for welding is 0.7 kJ, the peak values of the currents flowing through the 4, 8 and 16-turn coils become about 41, 21 and 11 kA, respectively. Since each rise time of the current and its generated magnetic flux (B) are almost the same, equivalent welding results can be obtained.

Keywords Welding, Al, Cu, Sheet, Magnetic pulse welding, Multi-turn flat coil, Capacitor bank, Series-discharge

1. Introduction

In recent years, the necessity of welding aluminum (Al) to copper (Cu) for electrical connection is increasing [1]. However, this welding is not easy due to the difference in physical quantities such as melting point. For this reason, a brittle intermetallic compound which is not suitable for welding may occur at the weld interface [2]. There are few efficient and excellent methods of the welding Al to Cu.

Magnetic (or electromagnetic) pulse welding belongs to impact welding similar to explosive welding, and recent review articles (including PhD thesis) have been reported [3-6]. Weld type is lap welding of various metal pairs [7-12]. The welding of Al/Cu has the greatest advantage of avoiding the formation of brittle intermetallic compounds. The weld interface of Al/Cu sheets shows wavy interface morphology like explosive welding [13-18]. The microstructure of the interface has been studied in detail and the high quality welds have been obtained [15-18]. The mechanism and features of Al/Cu sheets welding are considerably well known.

Its technique is based on discharging the current from the capacitor bank through the flat coil. Al/Cu sheets overlapped with a gap between them are fixed on the insulated coil. After the discharge, the magnetic flux (B) is suddenly generated around the coil. Strong electromagnetic forces act on the Al

sheet near the coil, the Al sheet collides with the upper Cu sheet and the both sheets are welded.

The peak discharge current required for welding was 140 to 230 kA using the conventional 1-turn flat coil and the 200 μF discharge capacitor bank [7]. The author have repeated experiments to reduce the high current using the multi-turn flat coil. For example, by using the 6-turn coil and the 24 μF capacitor bank, the peak current required for welding was reduced to about 1/6 as compared with the 1-turn coil [19-21]. In the future, such welding experiments with various multi-turn coils are expected to become popular.

In this report, the discharge bank capacity is chosen as 24, 6 and 1.5 μF for the 4, 8 and 16-turn coils respectively. Such three combinations in the welding of Al/Cu sheets are compared and examined. At the same discharge energy, the peak discharge current flowing to each coil decreases to about 1/2 when the number of turns is doubled. Since the rise time of each discharge current and its generated magnetic flux (B) can be made almost the same, experimental results equivalent to each other will be obtained. In order to reduce the discharge capacity without increasing the present charging voltage, after two or four same capacitors are charged in parallel, and then they are discharged in series to the 8 or 16-turn coil, respectively.

2. Welding method and discharge circuits

2.1 Welding method using multi-turn flat coil

Figure 1 is a schematic diagram of the 8-turn coil as an example. The coil consists of 8 E-shaped Cu alloy plates which are electrically insulated and are laminated. The discharge current flows into the narrow central part of the plate No.1 upward and flows out from the two wide outside parts downward. The divided currents join at the lower parts of the plate No.1. The joined current flows again into the central part of the plate No.2. The discharge current flows through each central part in series and does 8 turns. Each central part of the plates is just piled up with the same width. The high-density magnetic flux is generated around the piled central part as the 8-turn coil. Therefore, if the coil design is appropriate, this coil can generate the magnetic flux of the same value by the current of about 1/8 in comparison with the 1-turn coil.

The welding method will be explained using the 8-turn coil. The Al/Cu sheets are fixed on the coil as shown in Fig. 2. The lower Al sheet is insulated in a DC manner from the coil, but there is electromagnetic coupling between them. When the discharge current from the capacitor bank flows into the coil, the magnetic flux is rapidly generated around the central part. The flux penetrates into the Al sheet and eddy currents pass through the Al sheet to hinder its further penetration. As a result, the electro magnetic force f acts on the Al sheet. The Al sheet is accelerated upward and collides with the upper Cu sheet at high speed as shown in Fig. 3. The collision place moves laterally with time and two metal jets are emitted [10]. The weld interface is cleaned by the emission of metal jets. The sheets are welded in two narrow weld zones (seam weld zones).

Such welding can also be done using 4 and 16-turn coils. At this time, the discharge current required for welding varies with the coil turn number.

Eddy currents (current density i), electromagnetic force f and magnetic pressure p (equivalent to electromagnetic force) are given by Eq. (1), (2) and (3), respectively.

$$\text{rot } i = -\kappa (\partial \mathbf{B} / \partial t) \quad (1)$$

$$\mathbf{f} = i \times \mathbf{B} \quad (2)$$

$$p = (B_o^2 - B_i^2) / 2\mu \quad (3)$$

Here, κ and μ are electrical conductivity and magnetic permeability of the Al sheet. \mathbf{B} is the magnetic flux (density). B_o and B_i are the horizontal components of \mathbf{B} on the lower and the upper side of the Al sheet in Fig. 2, respectively.

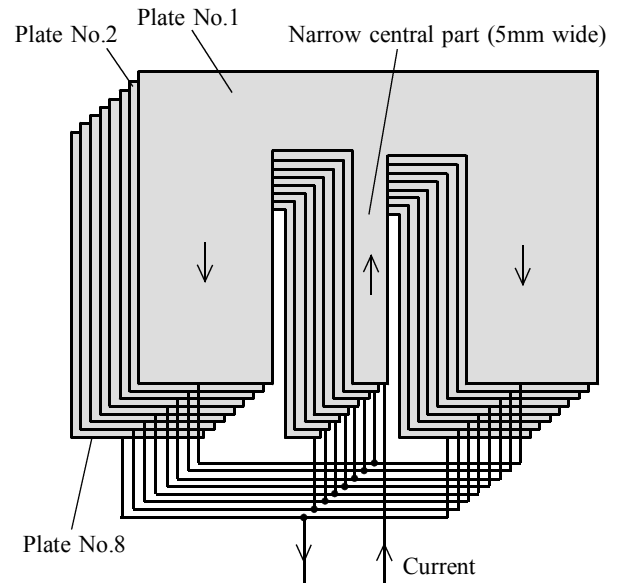


Fig. 1 Schematic diagram of 8-turn flat coil which consists of 8 E-shaped Cu alloy plates.

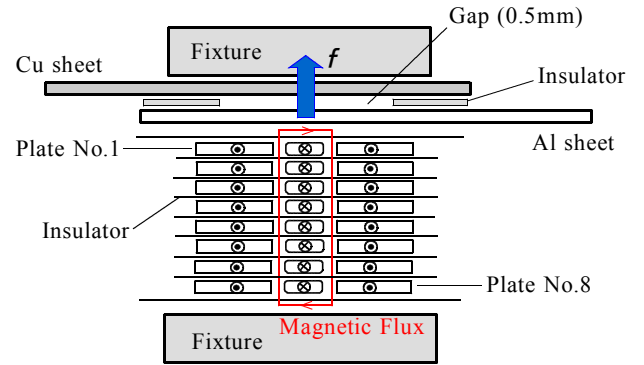


Fig. 2 Fixation of coil and Al/Cu sheets, and electromagnetic force f acting on Al sheet (sectional view).

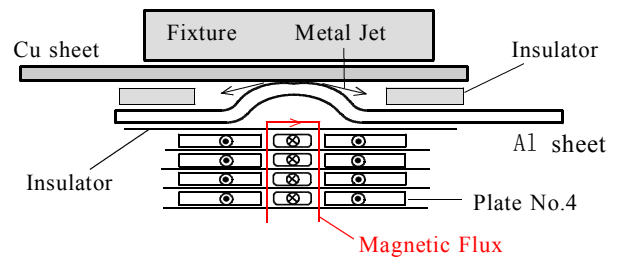
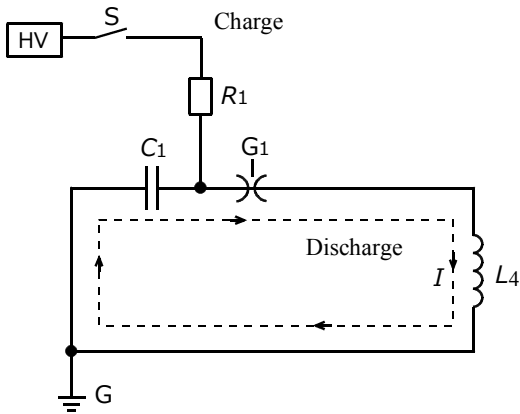


Fig. 3 Illustration immediately after collision of sheets and emission of metal jets (sectional view).

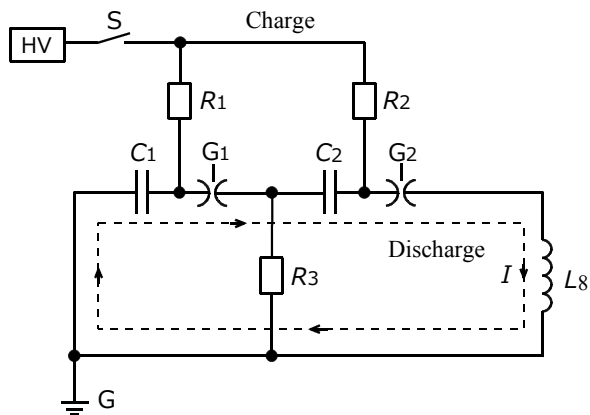
2.2 Discharge circuits

Figures 4, 5 and 6 show the circuit diagrams of the apparatus for charging and discharging each capacitor bank. The bank of Fig. 4 is normally charged and discharged. The banks of Figs. 5 and 6 are charged in parallel and discharged in



C_1 is capacitor ($24 \mu\text{F}$)
 G_1 is discharge spark gap switch
 L_4 is 4-turn coil
 R_1 is are resistor ($100 \text{ k}\Omega$)
 I is discharge current
 HV is high voltage DC power supply
 S is mechanical opening/closing switch
 G is ground (or earth)

Fig.4 Normally charging and discharge circuit diagram from capacitor bank to 4-turn coil.

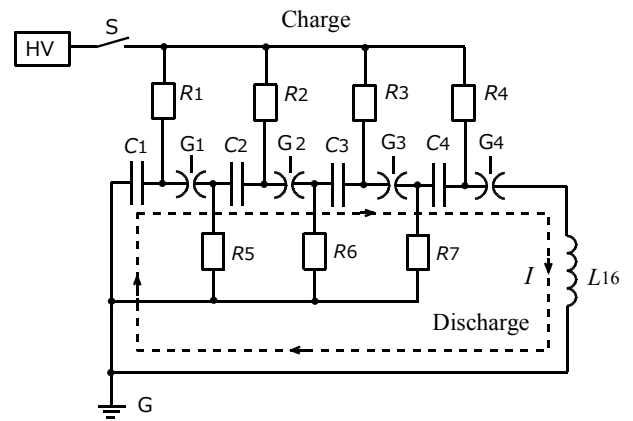


C_1, C_2 are capacitors ($12 \mu\text{F}$)
 G_1, G_2 are discharge spark gap switches
 L_8 is 8-turn coil
 R_1, R_2, R_3 are resistors ($100 \text{ k}\Omega$)
 I is discharge current
 HV, S and G are the same as in Fig. 4

Fig.5 Parallel-charging series-discharge circuit diagram from capacitor bank to 8-turn coil.

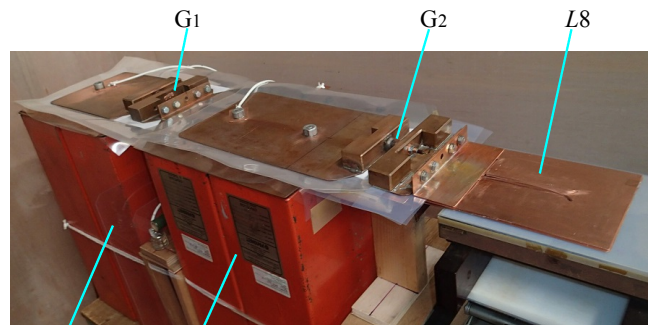
series. The 4, 8 and 16-turn coils are connected to each circuit diagram respectively. We ignore the discharge circuit resistance.

First, all the capacitors (C_1 etc.) of each discharge circuit are charged normally or in parallel using a high voltage DC power supply. Next, after the switch S is opened, the discharge



C_1, C_2, C_3, C_4 are capacitors ($6 \mu\text{F}$)
 G_1, G_2, G_3, G_4 are discharge spark gap switches
 L_{16} is 16-turn coil
 $R_1, R_2, R_3, R_4, R_5, R_6, R_7$ are resistors ($100 \text{ k}\Omega$)
 I is discharge current
 HV, S and G are the same as in Fig. 4

Fig.6 Parallel-charging series-discharge circuit diagram from capacitor bank to 16-turn coil.



C_1 ($12 \mu\text{F}$) C_2 ($12 \mu\text{F}$)

Fig. 7 Appearance of parallel charge series discharge circuit from capacitor bank to 8-turn coil.

gap switches (G_1 etc.) are triggered simultaneously, each capacitor discharges normally or in series, and the discharge current (I) flows through the discharge circuit along the dotted line. The discharge current (I) hardly flows into the charging circuit and ground circuit (including $100 \text{ k}\Omega$ resistor) of each capacitor bank. In Figures 4, 5 and 6, the discharge bank capacity is $24, 6$ and $1.5 \mu\text{F}$ respectively.

3. Experimental apparatus and materials

Figure 7 shows the appearance of the discharge circuit using the 8-turn coil without the upper fixture as an example. Each $12 \mu\text{F}$ capacitor consisted of two $6 \mu\text{F}$ capacitors in parallel. The capacitors, switches and the coil were placed as

close as possible to reduce the inductance of the transmission lines. The voltage during parallel charging was about 7.6 kV, and after series discharge, the capacity of the bank was 6 μF , the discharge energy was 0.7 kJ, and the total voltage during discharge was about 15 kV. The welding process was finished in one shot of series discharge. By triggering two gap switches at the same time, the series discharge stabilized.

The discharge current signal and a collision time signal of the sheets were obtained by using a measuring system as shown in Fig. 8.

The apparatus using the 4-turn coil consisted of the two capacitors (12 μF) of Fig. 7 connected in parallel to one capacitor bank (24 μF). The apparatus using the 16-turn coil consists of two capacitors (12 μF) in Fig. 7 divided into four capacitors (6 μF). Each capacitor (6 μF) are charged in parallel and discharged in series. The discharge capacity of this bank is 1.5 μF .

The material of the coil plates is, for example, a copper alloy C7025 having a conductivity of 45% and a tensile strength of 744 N/mm². In order to prevent deformation of the 16-turn coil plates (0.15mm thick), it is better to lower the conductivity and increase the tensile strength. The thickness of the polyimide sheet that insulates each plate of the 16-turn coil is 25 μm , and several polyimide sheets are used in a stack. This also reduces the total coil thickness.

The Al (1050) and Cu (1220) sheets were 100 mm long, 100 mm wide and 0.4 mm thick. The sheets were overlapped by 50 mm with the gap of 0.5 mm and fixed on the coil as shown in Fig. 2.

4. Experimental results

4.1 Discharge current and collision time signals

Typical discharge current and collision time signals when the 8-turn coil is used are shown in Fig. 9. In both signal waveforms, discharge noise occurred greatly at the beginning of the discharge, and small noise occurred thereafter. The damped oscillating current flowed through the coil during about 100 μs . In measurement the oscillating period was 23 μs . The inductance of the 8-turn coil was about 2.2 μH , which was about 55 times the inductance of the conventional 1-turn coil. When the discharge energy was 0.7 kJ, the peak discharge current was 21 kA, and the peak magnetic flux density B was about 15 T. The sheets collided at the peak current (4.0 μs from

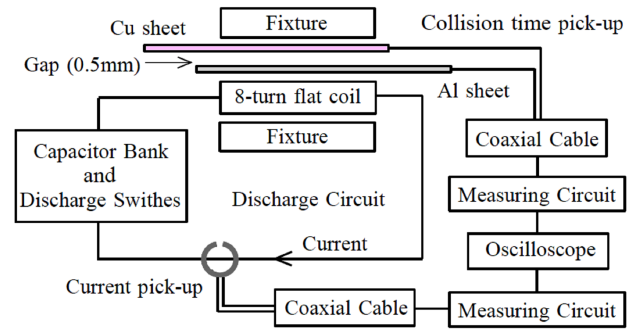


Fig. 8 Block diagram of discharge and measuring system using 8-turn coil.

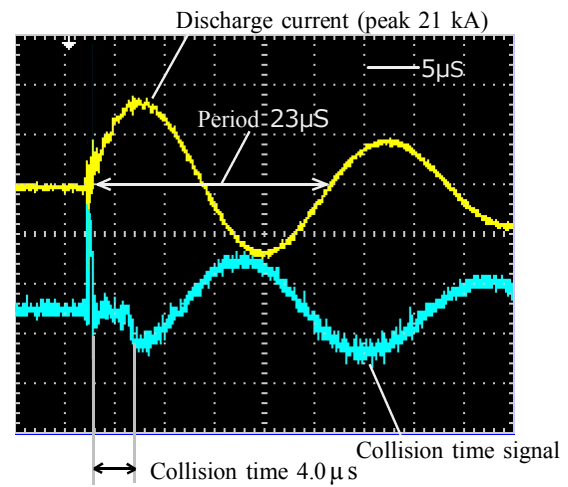


Fig. 9 Discharge current and collision time signals when discharge energy is 0.7 kJ and 8-turn coil is used.

the start of current). The collision speed when the sheets collided was calculated roughly with 250 m/s.

4.2 Appearance of welded Al/Cu sheets

Figure 10 shows a cross-sectional appearance of the Al/Cu sheets welded using the 8-turn coil. The lower Al sheet was deformed and welded to the upper Cu sheet as shown in Fig. 10. Two weld zones marked by arrows (\downarrow) and a middle clearance (non-weld zone) were seen. This result was similar to the case using 1, 4, and 6 turn coils [19-22]. Figure 11 is an example of the SEM image in the one weld zone. Wavy interface morphology like explosive welding was observed in two weld zones. Such a wavy interface was obtained using the 1, 4 and 6-turn coils [19-22]. Reasons for the occurrence of wavy interface are explained elsewhere [23]. High quality welds would have been obtained.

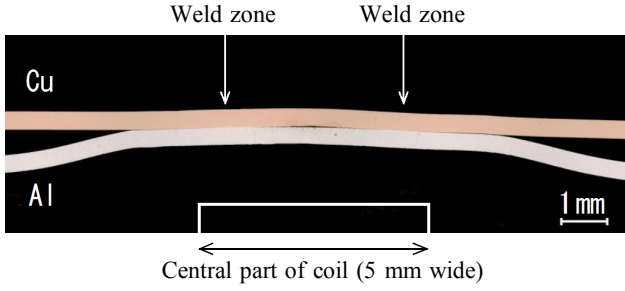


Fig. 10 Cross-sectional appearance of Al/Cu sheets welded using 8-turn coil and 0.7 kJ discharge energy.

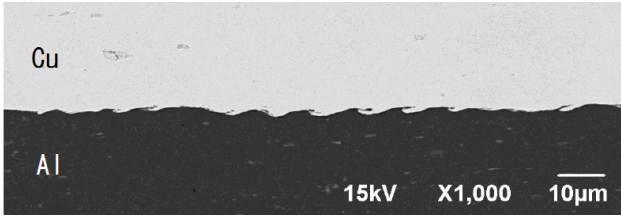


Fig. 11 SEM image of weld interface in one weld zone of Fig. 10.

5. Comparison and discussion of discharge to 4, 8 and 16-turn coils

Experimental results (including estimation) using the 4, 8 and 16 turn coils are compared and discussed. Table 1 shows comparison of the bank capacity at discharge, the oscillating period and the rise time of discharge current, the coil inductance, the peak current and the discharge energy for welding, approximate values of coil thickness, and the coil plate thickness. The period, the rise time and the peak current in Table 1 were obtained from measured current waveforms (for example Fig. 9). The values in Table 1 are approximate experimental values during welding. However, values of the row of 16-turn coil is estimated values.

In general, the damped oscillating period T of the discharge current in the series discharge circuit composed of a resistance R , a inductance L and a bank capacitance C is approximately given by Eq. (4) when $R \ll \sqrt{4L/C}$.

$$T = 2\pi\sqrt{LC} \quad (4)$$

Here, the condition of $R \ll \sqrt{4L/C}$ holds. The residual inductance (less than 0.04 μH) of each discharge circuit is sufficiently smaller than the inductance of each coil. The appearance of each coil is approximately same. So the period of the current is almost the same and the inductance of the 16-turn coil is about 4 times that of the 8-turn coil and current flowing through the 16-turn coil is half that of the 8-turn coil.

In the row of 4-turn of Table 1, if the discharge energy is

Table 1 Comparison of discharge to 4, 8 and 16-turn coils

Number of coil turns	4	8	16
Bank capacity at discharge (μF)	24	6	1.5
Oscillating period (μs)	24	23	23
Rise time of discharge current (μs)	3.2	3.3	3.3
Coil inductance (μH)	0.59	2.2	8.0
Peak current (kA)	31	21	11
Discharge energy (kJ)	0.4	0.7	0.7
Approximate coil thickness (mm)	3	4	4
Coil plate thickness (mm)	0.50	0.30	0.15

not 0.4 kJ but 0.7 kJ, the peak current value is 41 kA in proportional calculation. When the experiments in Table 1 are done with the energy of 0.7 kJ, peak current values flowing through the 4, 8 and 16-turn coils are expected to be 41 kA, 21 kA and 11 kA, respectively. The oscillating period and rise time of the discharge current are almost the same. The appearance of each coil is also the same. Therefore, if the discharge current of 11 kA is passed through the 16-turn coil, the same welding results as the experiments using the 4-turn and 8-turn coils will be obtained.

6. Conclusions

In this paper, the three combinations in magnetic pulse welding of Al/Cu sheets were compared and examined. Each capacitor bank of 24, 6 and 1.5 μF discharges into the 4, 8 and 16-turn coils, respectively. The oscillating period and the rise time of the discharge current flowing through each coil were almost the same, and the appearance of each coil was also the same. The following is expected at the same discharge energy.

(1) The peak discharge current flowing to each coil decreases to about 1/2 when the number of turns is doubled and the same high-density magnetic flux is generated in the same manner in the narrow central part of each coil.

(2) The welding results by each coil are almost the same and the three combinations are electrically equivalent.

(3) Such equivalent combinations are also possible with 24, 6 and 1.5 μF capacitors, and 5, 10 and 20-turn flat coils.

References

- [1] P. Bergmann, F. Petzoldt, R. Schuerer, S. Shneider: "Solid-state welding of aluminum to copper", *Welding in the World*, Vol. 157, No. 4, pp. 541-550, 2013.
- [2] P. Kar, C. Vimalraj, J. Martikainen, R. Suoranta: "Factors influencing Al-Cu weld properties by intermetallic compound formation", *International Journal of Mechanical and Materials Engineering*, Vol. 10, No. 10, pp. 1-13, 2015.
- [3] Y. Zhang: "Investigation of Magnetic Pulse Welding on Lap Joint of Similar and Dissimilar Materials", PhD Thesis, The Ohio State University, Columbus, USA, 2010.
- [4] A. Jassim: "Magnetic Pulse Welding Technology", *Iraq Journal of Electrical and Electronic Engineering*, Vol. 7, No. 2, pp. 169-179, 2011.
- [5] A. Kapil, A. Shama: "Magnetic Pulse Welding: an efficient and environmentally friendly multi-material joining technique", *Journal of Cleaner Production*, Vol. 100, pp. 35-58, 2015.
- [6] K. Shanthala, T. N. Sreenivasa: "Review on electromagnetic welding of dissimilar materials", *Frontiers of Mechanical Engineering*, Vol. 11, pp. 363-373, 2016.
- [7] V. Shribman, A. Stern, Y. Livshitz, O. Gafri, "Magnetic pulse welding produces high-strength aluminum welds", *Welding Journal* Vol. 81, pp.33-37, 2002.
- [8] T. Aizawa, M. Kashani, K. Okagawa: "Application of Magnetic Pulse Welding for Aluminum Alloys and SPCC Steel Sheet Joints", *Welding Journal*, Vol. 86, pp.119s-124s, 2007.
- [9] S. D. Kore, P. P. Date, S. V. Kulkarni: "Effect of process parameters on electromagnetic impact welding of aluminum sheets", *International Journal of Impact Engineering*, Vol. 34, pp. 1327-1341, 2007.
- [10] M. Watanabe, S. Kumai, K. Okagawa, T. Aizawa: "In-situ Observation of Magnetic Pulse Welding Process for Similar and Dissimilar Lap Joints Using a High-Speed Video Camera", *Aluminium Alloys*, Vol. 2, pp. 1992-1997, 2008.
- [11] A. Berlin, T. Nguyen, M. Worswick, Y. Zhou: "Metallurgical analysis of magnetic pulse welds of AZ31 magnesium alloy", *Science and Technology of Welding and Joining*, Vol. 16, pp. 728-734, 2011.
- [12] T. Aizawa, K. Okagawa, M. Kashani: "Application of magnetic pulse welding technique for flexible printed circuit boards (FPCB) lap joints", *Journal of Materials Processing Technology*, Vol. 213, pp. 1095-1102, 2013.
- [13] T. Aizawa, M. Yoshizawa: "Impulse magnetic pressure seam welding of Aluminum and Copper sheets", *Proc. 7th Int. Symp. of Japan welding Society*, Kobe, Japan, pp. 295-300, 2001.
- [14] T. Aizawa: "Fundamental Experiments for Magnetic Pulse Welding of Electric and Electronic Parts", *IEICE Technical Report*, Vol. 112, No. 370, EMD2012-92, pp. 7-12, 2012.
- [15] M. Watanabe, S. Kumai, T. Aizawa: "Interfacial microstructure of magnetic pressure seam welded Al-Fe, Al-Ni and Al-Cu lap joints", *Materials Science Forum*, Vol. 519-521, pp. 1145-1150, 2006.
- [16] Y. Zhang, S. Babu, G. Daehn: "Interfacial Ultrafine Grained Structures on Aluminum Alloy 6061 and Copper Alloy 110 Joint Fabricated by Electromagnetic Pulse Welding", *Journal of Materials Science*, Vol. 45, pp. 4645-4651, 2010.
- [17] T. Itoi, A. Mohamad, R. Suzuki, K. Okagawa: "Microstructure evolution of a dissimilar junction interface between an Al sheet and a Ni-coated Cu sheet joined by magnetic pulse welding", *Materials Characterization*, Vol. 118, pp. 142-148, 2016.
- [18] I. Kwee, K. Faes: "Interfacial Morphology and Mechanical Properties of Aluminium to Copper Sheet Joints by Electromagnetic Pulse Welding", *Key Engineering Materials*, Vol. 710, pp. 109-114, 2016.
- [19] T. Aizawa: "Magnetic Pulse Welding of Al/Cu Sheets using 6-Turn Flat Coil", *Proc. 10th Int. Conf. on Trends in Welding Research*, Tokyo, Japan, pp. 964-967, 2016.
- [20] T. Aizawa: "Magnetic Pulse Seam Welding of Al/Cu Sheets using 6-Turn Flat Coil", *IEICE Technical Report*, Vol. 116, No. 135, EMD2016-22, pp. 31-36, 2016.
- [21] T. Aizawa: "Improvement of 6-Turn Flat Coil for Magnetic Pulse Sheet-Welding", *Journal of Light Metal Welding*, Vol. 55, No. 3, pp. 95-100, 2017.
- [22] T. Aizawa: "Comparison of Al/Cu sheets welded by one-turn and four-turn flat coils for magnetic pulse welding", *IEICE Technical Report*, Vol. 117, No. 254, EMD2017-38, pp.1-6, 2017.
- [23] A. Ben-Artzy, A. Stern, N. Frage, V. Shribman, O. Sadot: "Wave formation mechanism in magnetic pulse welding", *International Journal of Impact Engineering*, Vol.37, pp. 397-404, 2010.